Published in final edited form as:
J Mol Cell Cardiol. 2013 September ; 62: 90–98. doi:10.1016/j.yjmcc.2013.04.016.

Functional roles of K_{ATP} channel subunits in metabolic inhibition

Alexey V. Glukhov[a,1], **Keita Uchida**[b,c,1], **Igor R. Efimov**[a], and **Colin G. Nichols**[b,c,*]

[a]Department of Biomedical Engineering, Washington University, St. Louis, MO 63130, USA

[b]Department of Cell Biology and Physiology, Washington University School of Medicine, 660 S. Euclid Avenue, St. Louis, MO 63110, USA

[c]Center for the Investigation of Membrane Excitability Diseases, Washington University School of Medicine, 660 S. Euclid Avenue, St. Louis, MO 63110, USA

Abstract

ATP-sensitive potassium channel (K_{ATP}) activation can drastically shorten action potential duration (APD) in metabolically compromised myocytes. We showed previously that SUR1 with Kir6.2 forms the functional channel in mouse atria while Kir6.2 and SUR2A predominate in ventricles. SUR1 is more sensitive to metabolic stress than SUR2A, raising the possibility that K_{ATP} in atria and ventricles may respond differently to metabolic stress. Action potential duration (APD) and calcium transient duration (CaTD) were measured simultaneously in both atria and ventricles by optical mapping of the posterior surface of Langendorff-perfused hearts from C57BL wild-type (WT; n = 11), Kir6.2$^{-/-}$ (n = 5), and SUR1$^{-/-}$ (n = 6) mice during metabolic inhibition (MI, 0 mM glucose + 2 mM sodium cyanide). After variable delay, MI led to significant shortening of APD in WT hearts. On average, atrial APD shortened by 60.5 ± 2.7% at 13.1 ± 2.1 min (n = 6, $p < 0.01$) after onset of MI. Ventricular APD shortening (56.4 ± 10.0% shortening at 18.2 ± 1.8 min) followed atrial APD shortening. In SUR1$^{-/-}$ hearts (n = 6), atrial APD shortening was abolished, but ventricular shortening (65.0 ± 15.4% at 25.33 ± 4.48 min, $p < 0.01$) was unaffected. In Kir6.2$^{-/-}$ hearts, two disparate responses to MI were observed; 3 of 5 hearts displayed slight shortening of APD in the ventricles (24 ± 3%, $p < 0.05$) and atria (39.0 ± 1.9%, $p < 0.05$) but this shortening occurred later and to much less extent than in WT ($p < 0.05$). Marked prolongation of ventricular APD was observed in the remaining hearts (327% and 489% prolongation) and was associated with occurrence of ventricular tachyarrhythmias. The results confirm that Kir6.2 contributes to APD shortening in both atria and ventricle during metabolic stress, and that SUR1 is required for atrial APD shortening while SUR2A is required for ventricular APD shortening. Importantly, the results show that the presence of SUR1-dependent K_{ATP} in the atria results in the action potential being more susceptible to metabolically driven shortening than the ventricle.

1. Introduction

ATP sensitive potassium channels (K_{ATP}) are activated in response to a reduced [ATP]/[MgADP] and hence couple metabolism to electrical activity [1,2]. K_{ATP} channels are densely expressed in the myocardium and when activated following metabolic inhibition can

*Corresponding author at: Department of Cell Biology and Physiology, Box 8228, Washington University School of Medicine, 660 S. Euclid Ave., St. Louis, MO 63110, USA. Tel.: +1 314 362 6630; fax: +1 314 362 7463. cnichols@wustl.edu (C.G. Nichols).
[1]These authors contributed equally.

Disclosures
None.

lead to significant shortening of the cardiac action potential and subsequent reduction of contractility [3, 4]. Activation of 1% of the total K_{ATP} expressed in the sarcolemmal membrane is sufficient to shorten action potential duration by 50% [5, 6]. In doing so, K_{ATP} activation is thought to play a cardioprotective role by conserving ATP.

Structurally, sarcolemmal K_{ATP} is a hetero-octameric channel formed from 4 regulatory sulfonylurea (SUR1, SUR2A or SUR2B) subunits and 4 pore forming, inwardly rectifying potassium channel (Kir6.1 or Kir6.2) subunits. Varying pharmacologic and functional properties arise from different K_{ATP} subunit compositions. The Kir subunits confer ATP, ADP, and PIP_2 sensitivity and determine the unitary conductance properties of the channel [7]. The regulatory SUR subunits positively modulate channel activity by responding to MgATP and MgADP, and are the target of inhibitory sulfonylurea drugs. Pharmacologically, both SUR1 and SUR2 are blocked by glibenclamide [8], while diazoxide and pinacidil are relatively selective activators of SUR1 and SUR2.

Previously, we have shown that murine cardiac K_{ATP} has a chamberspecific subunit composition; ventricular channels are primarily composed of SUR2A and Kir6.2 while atrial K_{ATP} is composed of SUR1 and Kir6.2 [8]. Following this discovery, we showed that this chamberspecific expression of K_{ATP} results in pharmacologically distinct responses of the action potential, with the atrial action potential duration (APD) showing strong shortening only when exposed to diazoxide and the ventricular APD shortening only in response to pinacidil [9].

SUR1 also has a higher sensitivity to stimulation by MgADP compared to SUR2A and thus has a greater sensitivity to metabolic stress [10] although in vivo consequences of this has thus far not been examined, and there have been no experiments looking at the function of these channels on intact hearts following metabolic stress. In the present study we have examined the consequences of chamber-specific SUR expression on the metabolic sensitivity of cardiac electrical activity by optical mapping in WT, SUR1 knockout and Kir6.2 knockout hearts in response to metabolic inhibition.

2. Materials and methods

2.1. Generation and care of genetically modified mice

All procedures complied with the standards for the care and use of animal subjects as stated in the *Guide of the Care and Use of Laboratory Animals* (NIH publication no. 85-23, revised 1996) and protocols were approved by the Animal Studies Committee at Washington University School of Medicine. Data were obtained from adult (aged 11 to 20 weeks) C57BL wild type mice (WT, n = 11), sulfonylurea receptor type 1 knockout mice ($SUR1^{-/-}$, n = 6) and Kir6.2 knockout mice ($Kir6.2^{-/-}$, n = 5). The generation of $SUR1^{-/-}$ and $Kir6.2^{-/-}$ mice has been described elsewhere [11,12].

2.2. Isolated heart preparations

The isolated heart preparation (Fig. 1A) was performed as described previously [9]. Briefly, mice were anesthetized using a mixture of Ketamine and Xylazine, with 100 units of heparin. After mid-sternal incision, the heart was removed and placed in oxygenated (95% O_2, 5% CO_2) modified Tyrode solution of the following composition: 128.2 mM NaCl, 4.7 mM KCl, 1.19 NaH_2PO_4, 1.05 mM $MgCl_2$, 1.3 mM $CaCl_2$, 20.0 mM $NaHCO_3$, and 11.1 mM glucose (pH = 7.35 ± 0.05). While bathed in the same solution, the lung, thymus, and fat tissue were dissected and removed. A short section of the aorta was attached to a custom made 21-gauge cannula. After cannulation, the heart was superfused and retrogradely perfused using a peristaltic pump (Peri-Star, WPI, Sarasota, USA) with Tyrode solution passed through a 5-μm filter (Millipore, Billerica, USA) and warmed (37°C) using a water

jacket and circulator (ThermoNESLAB EX7, Newtown, USA). Perfusion was performed under constant aortic pressure of 60 to 80 mm Hg, monitored by a pressure-amplifier (TBM4M, WPI, Sarasota, USA).

The isolated heart was pinned at the apex to the Sylgard bottom of the chamber to prevent stream-induced movement. The right (RA) and left (LA) atrial appendages were stretched and pinned to flatten them and to allow optical measurements from maximal surface of the atria (Fig. 1A). A small silicon tube, fixed by silk to nearby connective tissue, was inserted into the left ventricle through the pulmonary vein, LA, and tricuspid valve to prevent solution congestion and subsequent ischemia after suppression of ventricular contractions. This also prevented acidification of the perfusion solution and development of ischemia in the left ventricle.

2.3. Imaging system

After the initial 20–30 min of perfusion, the heart was immobilized by inclusion of blebbistatin (10–20 μM, Tocris Bioscience, Ellisville, MO) in the perfusion medium in order to suppress motion artifacts in optical recordings [13]. For all hearts, the tissue was stained via coronary perfusion for 10–20 min with voltage-sensitive dye RH237 (5 μL of 1.25 mg/mL solution in DMSO, Invitrogen, Carlsbad, CA). For 5 of 11 WT and all $SUR1^{-/-}$ and $Kir6.2^{-/-}$ hearts, the tissue was co-stained with calcium indicator Rhod-2 AM (20 μL of 1 mg/mL solution in DMSO, Invitrogen, Carlsbad, CA) for simultaneous mapping of action potential and calcium transient.

Two halogen lamps (Newport Oriel Instruments, Stratford, CT; SciMedia, Costa Mesa, CA), equipped with 520 ± 45 nm bandpass filters were used for excitation. Fluorescent voltage and calcium signals were simultaneously collected from the same field of view. Fluorescence emission was separated by a dichroic mirror (635 nm cutoff, Omega Optical, Brattleboro, VT), and filtered by a 700 nm longpass filter (Thorlabs, Newton, New Jersey) for voltage signals and by a 590 (±15) nm bandpass filter (Omega Optical, Brattleboro, VT) for calcium signals. Emitted light was then recorded by a dual CMOS camera system (ULTIMA-L, SciMedia, Costa Mesa, CA) with high spatial (100 × 100 pixels, 110 ± 20 μm per pixel) and temporal (500–1000 frames/s) resolution. The acquired fluorescence signal was digitized, amplified, and visualized using custom software (SciMedia, Costa Mesa, CA).

2.4. Experimental protocols

After isolation and cannulation, motion suppression, and dye staining, preparations were equilibrated for an additional 5–10 min before imaging of control measurements during spontaneous rhythm and ventricular pacing. The pacing site was located on the lateral, anterior right ventricular (RV) epicardium near the apex; pacing current was at least 2× the pacing threshold. After control measurements, hearts were exposed to complete metabolic inhibition (MI). The control Tyrode solution used for perfusion was switched to a solution with 2 mM NaCN and zero glucose. Cyanide was added to inhibit oxidative phosphorylation; the absence of glucose resulted in inhibition of glycolysis [14]. Cyanide was dissolved immediately before use to minimize loss of HCN gas from the solution. Optical measurements, during both spontaneous rhythm and ventricular pacing, were taken frequently (~ every minute) in order to maximize time sampling to observe action potential and calcium transient changes.

Once perfusion of the MI solution began, there was a variable time course for the onset of the effect of MI due to variability in perfusion rate and metabolic state of each heart prior to the start of the experiment. In a typical experiment, the sinus rhythm would slow and

progressive conduction block would develop between the atria and ventricle, prior to the onset of APD changes in the atrial or ventricular myocardium, suggesting high susceptibility of the conduction system to the effects of MI. Once complete anterograde AV block occurred, files with ventricular pacing were preferentially obtained to monitor APD changes. Cyanide induced progressive inhibition of cardiac activity and optical recordings were taken until the ventricular myocardium became inexcitable.

2.5. Data processing

A customized Matlab-based computer program was used to analyze the optical signals and detailed processing methods are reviewed elsewhere [15]. Briefly, signals were filtered using a low-pass Butterworth filter algorithm (f_c = 200 Hz). Maximum upstroke derivative (dV/dt_{max}) was calculated for each action potential using the normalized optical signal and its derivatives. Activation maps (Fig. 1B) were constructed from activation times, which were determined from dV/dt_{max}. Conduction velocity (CV) was defined as the distance traveled by the wave front per unit time. To characterize cardiac repolarization, the mean APD at 80% of repolarization (APD) was calculated during continuous pacing for each channel and then averaged throughout the corresponding chamber (RA, LA, RV and LV). Similarly, calcium transient durations (CaTD) were measured at 80% return to baseline fluorescence and averaged throughout the chambers.

2.6. Statistical analysis

Values are expressed as means ± SE unless otherwise stated. Hypothesis testing was carried out using unpaired Student's t-test and chi-squared analysis with Yates correction, as appropriate. A value of $p < 0.05$ was considered statistically significant.

3. Results

3.1. Dual voltage-calcium imaging of murine hearts

Prior to the start of MI, control measurements were taken in both sinus rhythm and during pacing from the lateral edge of the ventricle (Fig. 1). The measured control APDs (Table 1) and CaTDs (Table 2) during control conditions are summarized for all groups. The APDs are similar to previously reported values [9], with no statistical differences between the three genotypes for control APDs or CaTDs in each chamber.

3.2. Atrial APD shortens before ventricular APD in WT mice hearts during MI

To monitor the effects of K_{ATP} activation on cardiac action potentials, action potential duration (APD) was measured throughout MI. As expected, MI was associated with a profound shortening of both the atrial and ventricular APDs, measured at 80% repolarization (APD_{80}), in the WT heart. Representative APD_{80} maps and optical action potentials from one WT heart are shown at three different time points during MI (Figs. 2A–B). During control, ventricular APD_{80} was ~60–70 ms in both chambers. By 11 min, a subtle prolongation of APD_{80} is evident across both ventricles but by 17 min, drastic shortening of the APD_{80} occurred in both. In each atrium, there is also clear APD_{80} shortening that occurs considerably faster (by 11 min), and by 17 min there is no detectable atrial activity. APD was also measured at 15% repolarization (APD_{15}). APD_{15} shortened slightly, but non-significantly with MI, in both WT and $SUR1^{-/-}$ ventricles but the majority of the APD shortening occurs late, in phase 3 of the action potential (as seen in Figs. 2B, 3B, and 4B). There was also no significant shortening of the atrial APD at 15% repolarization.

Similar progression was observed in all 11 WT hearts although there was highly variable delay to onset of APD_{80} changes suggesting that there is variability in the initial metabolic state of the heart. However, once initiated, the progression was remarkably similar. In all

WT hearts, the right atrial APD_{80} shortened prior to the right ventricular APD; 50% shortening of the atrial APD_{80} occurred at 13.1 ± 2.1 min after onset of MI (Fig. 2C). The ventricles displayed 50% shortening of APD_{80} approximately 5 min after the atrial APD_{80} shortening at 18.2 ± 1.8 min after onset of MI ($p < 0.01$).

To focus on the relationship between atrial and ventricular APD shortening, in Fig. 2C the time axes are referenced to the time of 50% shortening of the ventricular APD (relative time (T_{rel}) = 0) to normalize for the variability in onset. This analysis makes clear that atrial APD shortening occurred between 10 and 2.5 min prior to ventricular APD shortening in every heart. Following maximal atrial APD shortening, atrial optical action potentials continued to shorten, but the signal amplitude also weakened until APD became unmeasurable. Since APD can show significant differences between the left and right hearts, the APD in the left atria and right atria was plotted against each other throughout MI (Fig. 2D). For each heart the APDs in LA and RA were strongly correlated throughout MI ($R^2 = 0.0.83$), as were the APDs in the left and right ventricles ($R^2 = 0.84$). We conclude that the effects of MI on LA and RA behaved similarly throughout MI and henceforth, the left and right atrial and ventricular APDs are grouped as merely atrial and ventricular APDs (Fig. 2E).

3.3. Chamber-specific ablation of K_{ATP} abolishes APD shortening in a chamber-specific manner

To determine whether the APD shortening that was observed during MI is due to specific K_{ATP} subunits, the above experiment was repeated in hearts from $SUR1^{-/-}$ and $Kir6.2^{-/-}$ mice. $SUR1^{-/-}$ hearts displayed similar changes in ventricular APD to WT hearts but essentially no shortening of the atrial APD (Figs. 3A–C). Figs. 3D and E summarize the APD changes and a clear, significant difference can be seen in the maximal shortening of the atrial APD (to 85% of control in $SUR1^{-/-}$ vs 43% in WT, $p < 0.01$). The lack of SUR1 did not affect the ventricular APD shortening (to 35% of control in $SUR1^{-/-}$ vs 34% in WT, p = NS). This suggests that SUR1 based K_{ATP} is indeed responsible for nearly all of the APD shortening observed during MI in the murine atria whereas SUR2 is likely responsible for APD shortening in the ventricle. In contrast, there was negligible APD shortening during MI in both atria and ventricles of $Kir6.2^{-/-}$ hearts (Figs. 4A–B). There was a moderate shortening in three out of five $Kir6.2^{-/-}$ atria very late in MI to 60 ± 4% of control APD but no atria showed APD shortening below 50% of control values. A similar, minimal, shortening to 76 ± 5% of control APD was observed in these ventricles ($Kir6.2^{-/-}$ #3–5) immediately before the myocardium became inexcitable. These results indicate that activation of Kir6.2-dependent K_{ATP} is responsible for a large portion of the APD shortening during MI in both atria and ventricle.

Intriguingly, two of five $Kir6.2^{-/-}$ mice (#1 and #2, Figs. 4A–C) displayed severe APD prolongation in the ventricles (327% and 489% compared to control APD) during MI. These hearts developed both ventricular tachycardia (VT+) and, through retrograde activation, atrial tachycardia, that was not terminated by stimulation (not shown). Development of VT occurred at ~17 min and ~16 min of MI for hearts #1 and #2 respectively.

Development of VT in the VT+ hearts was observed during progressive prolongation of ventricular APD and seemed to be associated with triggered activity originating from a focal point near the base of the ventricle. Fig. 4D shows an example of VT recorded in $Kir6.2^{-/-}$ heart #1. During tachycardia in this heart there was progressive prolongation of APD and decrease of the optical signal amplitude until the signal became undetectable. The extreme APD prolongation in these two VT+ $Kir6.2^{-/-}$ hearts was accompanied by CaTD prolongation which was not observed in the three VT – $Kir6.2^{-/-}$ hearts (Fig. 4E).

Severe CaTD prolongation was not observed in any of the other hearts. Representative AP and CaT traces are shown for one WT heart (Fig. 5A). Atrial APD is shorter than the atrial CaTD in all groups whereas APD and CaTD in control ventricles are very similar (Tables 1, 2, Fig. 5A: Control). In WT (n = 5), $SUR1^{-/-}$ (n = 6), and the remaining VT− $Kir6.2^{-/-}$ atria and ventricles, CaT duration (CaTD) remains relatively stable throughout MI in both atria and ventricle (Figs. 5B–C). Maximum prolongation and subsequent maximum shortening of the CaTD is quantified in Figs. 5D and E. Slight prolongation of CaTD and subsequent minimal shortening roughly paralleled the changes in APD, suggesting minimal additional effects of MI on the kinetics of calcium handling.

4. Discussion

4.1. Chamber specificity of K_{ATP} channel structure and functional consequences

Progress in understanding cardiac K_{ATP} channels has suffered under the persistent dogma that these channels are of uniform composition (Kir6.2 and SUR2A) and expression. Here we provide further evidence that there are regional differences in K_{ATP} subunit expression in the murine heart and we show that in intact hearts the different channel compositions confer temporally separated response to metabolic stress. Firstly, the present study provides additional evidence supporting our previous findings that Kir6.2 co-expresses with SUR1 in the atria and SUR2A in the ventricle in murine hearts [8,9] by demonstrating that APD shortening is abolished specifically in the atria of $SUR1^{-/-}$ hearts, suggesting that these K^+ channels are the main driver of APD shortening following metabolic stress in mice. Ventricular APD shortening remained unaffected in $SUR1^{-/-}$ hearts, consistent with canonical SUR2A-based K_{ATP} channels remaining active in the ventricle. Surprisingly, the three VT− $Kir6.2^{-/-}$ hearts still showed some APD shortening in late MI in both atria and ventricle. There has been some evidence to suggest that Kir6.1 may be expressed in the heart [16–18] and it is plausible that the APD shortening observed in the $Kir6.2^{-/-}$ hearts may be due to Kir6.1-based K_{ATP} activity. However, it is also likely that I_{Ca} is reduced late in MI and that this underlies the late shortening and further studies will be needed to fully determine the etiology of late APD shortening in the $Kir6.2^{-/-}$ hearts.

Importantly, we observed atrial APD shortening in all WT hearts prior to ventricular APD shortening, suggesting that the K_{ATP} composition in the atria and ventricle confers different responses to metabolic inhibition. Such a functional consequence is actually predicted by previous biophysical and biochemical analyses which indicate that nucleotide binding folds (NBFs) of SUR1 display a greater sensitivity to nucleotide diphosphate activation than the SUR2A NBFs [10]. Due to this difference at the molecular level, SUR1 based K_{ATP} is predicted to have greater sensitivity to activation by metabolic stimuli than SUR2A based K_{ATP} [10], leading to the expectation that SUR1 based K_{ATP} channels will activate more readily than SUR2A based K_{ATP} channels during hypoxia, ischemia, or MI in the heart. In our analysis of SUR-dependence of atrial and ventricular K_{ATP} [19], we observed spontaneous activation of K_{ATP} channels in atrial myocytes under whole cell conditions with 0 or 500 μM MgATP in the pipette while ventricular myocytes require agonists or metabolic inhibition for K_{ATP} channel activation. This is consistent with a previous report that cultured neonatal rat atrial myocytes exhibited greater K_{ATP} activation than ventricular myocytes when patch clamped with a high [ADP]/[ATP] pipette solution [20]. Using transgenic overexpression of nonfunctional αMHC-Kir6.1 [AAA] channels, Zhu et al. reduced the K_{ATP} channel current density by approximately 80% and demonstrated that reduced functional channels slowed the time course of APD shortening during hypoxia [21]. Our study now confirms in the intact heart, more metabolically-sensitive SUR1-based K_{ATP} channels activate earlier than SUR2A based K_{ATP} channels during MI.

4.2. Effect of K_{ATP} activation on APD and its potential role in arrhythmogenesis

A large body of literature exists describing the arrhythmogenic role that K_{ATP} activation can play and the potential for K_{ATP} channel blockers such as glibenclamide for use as antiarrhythmic agents [22,23]. Activation of K_{ATP} could be expected to shorten both atrial and ventricular APDs and refractory periods, thereby preparing the tissue for re-entry by reducing the wavelength of re-entry [24,25] in larger hearts. Although re-entrant arrhythmias were not observed in our study of mouse hearts, the current study may help to explain why SUR1 overexpression in mice has been associated with a variety of arrhythmias, including atrioventricular block and atrial tachycardia, whereas SUR2A overexpression has not [26]. The greater potential for APD shortening by SUR1-based K_{ATP} during milder metabolic stresses such as during exercise or fasting may suggest that this might be the more important subunit to study for the arrhythmogenicity of K_{ATP} channels.

However, as shown previously [27,28], in early myocardial ischemia or hypoxia there can be opposite changes in refractoriness and APD, which may indicate that K_{ATP} activation during ischemic conditions will not necessarily be arrhythmogenic or damaging; indeed activation of cardiac K_{ATP} channels has consistently been shown to protect the heart from damage during ischemia, by limiting Ca^{2+} entry [2]. In a study of rabbit atria, a transient increase in refractory period of about 30% was observed in the first 20 min of hypoxia. In contrast, the APD decreased monotonically from 100% to 72% at 30 min of hypoxia, suggesting the development of postrepolarization refractoriness [27]. Transient postrepolarization refractoriness could be due to different rates of changes in APD and sodium channel kinetics and may protect against both reentrant arrhythmias and arrhythmias triggered by EADs in early MI.

Lack of K_{ATP} activation might actually precipitate arrhythmias during MI. Although we observed single isolated and non-sustained EADs in 1 WT and in 1 $SUR1^{-/-}$ ventricle prior to APD shortening, the predominant sustained arrhythmic feature was focal activity, of unknown etiology, in $Kir6.2^{-/-}$ ventricles. In these ventricles, a significant APD prolongation was observed in the early phase of MI, in agreement with the transient APD prolongation revealed previously by Saito et al. during the early phase of ischemia in $Kir6.2^{-/-}$ mouse ventricles [29]. These authors made the reasonable suggestion that inhibition of other potassium currents (such as I_{to} and I_{K1}) by metabolites as well as an increase in intracellular Ca^{2+} might lead to the observed APD prolongation, and may precipitate EADs or DADs leading to sustained focal arrhythmias n $Kir6.2^{-/-}$ hearts in the present study.

The sinus rate in $Kir6.2^{-/-}$ hearts maintains a short cycle length during hypoxia [30] and it is conceivable that Kir6.2 may normally play a role in slowing pacemaker rates in the AV node and His-Purkinje system. The origin of the trigger cannot be determined from epicardial optical mapping preparations, and the role of His-Purkinje pacemakers cannot be excluded. Diastolic intracellular calcium-voltage coupling has been shown to be higher in the endocardium and Purkinje fibers compared to the epicardium [31] and a depolarized membrane potential compounded with the loss of Kir6.2 may generate a substrate for DADs. Therefore, the focal activity that was observed in our study (Fig. 4) may result from EAD- or DAD-driven propagation of APs into the epicardium through the region with the shortest refractoriness. There are reports that $Kir6.2^{-/-}$ mice or mice expressing a dominant-negative mutated Kir6.2 subunit have calcium handling deficiencies that can lead to calcium overload in these hearts [32,33]. These studies further suggest that the observed arrhythmias in the $Kir6.2^{-/-}$ hearts may be due to calcium-mediated triggered activity in the ventricular myocardium. These observations and other insights from the literature support a generally accepted consensus that a major function of K_{ATP} channels during metabolic stress is to reduce Ca^{2+} entry by minimizing membrane depolarization, limiting contraction, and

conserving energy [34,35] and the loss of this hyperpolarizing current may exacerbate calcium entry into the cell.

4.3. Clinical implications

Despite the clear chamber specificity in rodents, other species exhibit varying sensitivities to SUR1 and SUR2A agonists in the atria and ventricles. Importantly, human cardiac chambers lack a distinct differential pharmacological response in atrial and ventricular K_{ATP} channels to diazoxide and pinacidil [36], consistent with K_{ATP} subunit gene expression pattern [23]. Although chamber-specific SUR expression is lacking in humans, recent work suggests that various disease states can affect K_{ATP} function and expression [37]. We previously noted a potentiation of diazoxide-sensitive K_{ATP} activity in explanted human hearts from patients diagnosed with congestive heart failure (CHF) and in patients with a non-failing heart but with a history of infarction compared to non-failing hearts [36]. However, the drastic pinacidil-induced APD shortening in both the atria and ventricles was unaffected by the disease state. Activation of K_{ATP} channels in explanted human hearts by both diazoxide and pinacidil led to both atrial and ventricular reentrant arrhythmias, which could be terminated by glibenclamide [36]. Although surface protein expression levels need to be addressed, this increased diazoxide-sensitive APD shortening may point to an increase in the functional number of SUR1-based K_{ATP} channels. In rat hearts, expression of Kir6.1 and all SUR regulatory subunits were increased up to 3-fold in cardiomyocytes located in the infarct border zone, 20 weeks after coronary occlusion [38]. Diazoxideactivated K_{ATP} currents were observed in these border zone cells, while there was no response to diazoxide in control ventricular cardiomyocytes, again suggesting that the activity and expression of SUR1 increases in ventricles following myocardial infarction in rats. In a mouse model of salt-induced hypertension, Lader et al. [24] demonstrated increased K_{ATP} channel density and upregulation of SUR1 subunit expression in atria, associated with an increased atrial arrhythmia inducibility. Koumi et al. demonstrated that K_{ATP} channels in atrial myocytes from patients with CHF have characteristics substantially similar to those in donors, but the channels were more sensitive to stimulation by metabolic inhibition in CHF myocytes than in donor myocytes [39]. These findings further suggest that K_{ATP} channel expression and/or sensitivity are plastic under different levels and durations of metabolic stress, such as during heart failure, which may be one explanation for the observed differences in effects of diazoxide between non-infarcted donor hearts and infarcted donor and CHF hearts. Finally, recent work by Farid et al. demonstrated regional disease-related expression of K_{ATP} channels in human cardiomyopathic hearts, consistent with the distribution of K_{ATP} expression being an important factor in its arrhythmogenicity [23]. K_{ATP} blockade by glibenclamide promoted termination of spontaneous ventricular tachyarrhythmia by attenuating the ischemia-dependent spatiotemporal heterogeneity of refractoriness. Further studies will be necessary to determine how various disease states can impact K_{ATP} subunit expression and to assess how these changes in K_{ATP} composition and distribution in the myocardium can influence the arrhythmogenic potential in these patients.

Acknowledgments

This work was supported by NIH grant HL95010 to CGN. We are grateful to Matt Sulkin for technical assistance and for providing an updated version of the Matlab based analysis GUI. We also thank Haixia Zhang for her helpful discussion and for critically reviewing the data and manuscript. Finally, we thank Drs. Susumu Seino for the Kir6.2$^{-/-}$ mice and Mark Magnuson for the SUR1$^{-/-}$ mice.

References

1. Noma A. ATP-regulated K + channels in cardiac muscle. Nature. 1983; 305(5930):147–148. [PubMed: 6310409]

2. Flagg, Thomas P.; Charpentier, F.; Manning-Fox, Jocelyn; Sara, Remedi Maria; Enkvetchakul, Decha; Lopatin, Anatoli, et al. Remodeling of excitation-contraction coupling in transgenic mice expressing ATP-insensitive sarcolemmal KATP chan-nels. Am J Physiol Heart Circ Physiol. 2003; 286(4):H1361–H1369. [PubMed: 14656703]
3. Nichols CG, Lederer WJ. The regulation of ATP-sensitive K + channel activity in intact and permeabilized rat ventricular myocytes. J Physiol. 1990; 423:91–110. [PubMed: 2388163]
4. Nichols CG, Lederer WJ. The role of ATP in energy-deprivation contractures in unloaded rat ventricular myocytes. Can J Physiol Pharmacol. 1990; 68(2):183–194. [PubMed: 2311000]
5. Lederer WJ, Nichols CG, Smith GL. The mechanism of early contractile failure of isolated rat ventricular myocytes subjected to complete metabolic inhibition. J Physiol. 1989; 413:329–349. [PubMed: 2600854]
6. Shaw RM, Rudy Y. Electrophysiologic effects of acute myocardial ischemia: a theoretical study of altered cell excitability and action potential duration. Cardiovasc Res. 1997; 35(2):256–272. [PubMed: 9349389]
7. Nichols CG. KATP channels as molecular sensors of cellular metabolism. Nature. 2006; 440(7083): 470–476. [PubMed: 16554807]
8. Flagg TP, Kurata HT, Masia R, Caputa G, Magnuson MA, Lefer DJ, et al. Differential structure of atrial and ventricular KATP: atrial KATP channels require SUR1. Circ Res. 2008; 103(12):1458–1465. [PubMed: 18974387]
9. Glukhov AV, Flagg TP, Fedorov VV, Efimov IR, Nichols CG. Differential K(ATP) channel pharmacology in intact mouse heart. J Mol Cell Cardiol. 2009; 48(1):152–160. [PubMed: 19744493]
10. Masia R, Enkvetchakul D, Nichols CG. Differential nucleotide regulation of KATP channels by SUR1 and SUR2A. J Mol Cell Cardiol. 2005; 39(3):491–501. [PubMed: 15893323]
11. Shiota C, Larsson O, Shelton KD, Shiota M, Efanov AM, Hoy M, et al. Sulfonylurea receptor type 1 knock-out mice have intact feeding-stimulated insulin secretion despite marked impairment in their response to glucose. J Biol Chem. 2002; 277(40):37176–37183. [PubMed: 12149271]
12. Miki T, Nagashima K, Tashiro F, Kotake K, Yoshitomi H, Tamamoto A, et al. Defective insulin secretion and enhanced insulin action in KATP channel-deficient mice. Proc Natl Acad Sci U S A. 1998; 95(18):10402–10406. [PubMed: 9724715]
13. Fedorov VV, Lozinsky IT, Sosunov EA, Anyukhovsky EP, Rosen MR, Balke CW, et al. Application of blebbistatin as an excitation-contraction uncoupler for electrophysiologic study of rat and rabbit hearts. Heart Rhythm. 2007; 4(5):619–626. [PubMed: 17467631]
14. Allen DG, Morris PG, Orchard CH, Pirolo JS. A nuclear magnetic resonance study of metabolism in the ferret heart during hypoxia and inhibition of glycolysis. J Physiol. 1985; 361:185–204. [PubMed: 3989725]
15. Laughner JI, Ng FS, Sulkin MS, Arthur RM, Efimov IR. Processing and analysis of cardiac optical mapping data obtained with potentiometric dyes. Am J Physiol Heart Circ Physiol. 2012; 303(7):H753–H765. [PubMed: 22821993]
16. Morrissey A, Parachuru L, Leung M, Lopez G, Nakamura TY, Tong X, et al. Expression of ATP-sensitive K + channel subunits during perinatal maturation in the mouse heart. Pediatr Res. 2005; 58(2):185–192. [PubMed: 16085792]
17. Bao L, Kefaloyianni E, Lader J, Hong M, Morley G, Fishman GI, et al. Unique properties of the ATP-sensitive K(+) channel in the mouse ventricular cardiac conduction system. Circ Arrhythm Electrophysiol. 2011; 4(6):926–935. [PubMed: 21984445]
18. Morrissey A, Rosner E, Lanning J, Parachuru L, Dhar Chowdhury P, Han S, et al. Immunolocalization of KATP channel subunits in mouse and rat cardiac myocytes and the coronary vasculature. BMC Physiol. 2005; 5(1):1. [PubMed: 15647111]
19. Glukhov AV, Flagg TP, Fedorov VV, Efimov IR, Nichols CG. Differential K(ATP) channel pharmacology in intact mouse heart. J Mol Cell Cardiol. 2010; 48(1):152–160. [PubMed: 19744493]
20. Poitry S, van Bever L, Coppex F, Roatti A, Baertschi AJ. Differential sensitivity of atrial and ventricular K(ATP) channels to metabolic inhibition. Cardiovasc Res. 2003; 57(2):468–476. [PubMed: 12566119]

21. Zhu Z, Burnett CM, Maksymov G, Stepniak E, Sierra A, Subbotina E, et al. Reduction in number of sarcolemmal KATP channels slows cardiac action potential duration shortening under hypoxia. Biochem Biophys Res Commun. 2011; 415(4):637–641. [PubMed: 22079630]
22. Billman GE. The cardiac sarcolemmal ATP-sensitive potassium channel as a novel target for anti-arrhythmic therapy. Pharmacol Ther. 2008; 120(1):54–70. [PubMed: 18708091]
23. Farid TA, Nair K, Masse S, Azam MA, Maguy A, Lai PF, et al. Role of KATP channels in the maintenance of ventricular fibrillation in cardiomyopathic human hearts. Circ Res. 2011; 109(11): 1309–1318. [PubMed: 21980123]
24. Lader JM, Vasquez C, Bao L, Maass K, Qu J, Kefalogianni E, et al. Remodeling of atrial ATP-sensitive K channels in a model of salt-induced elevated blood pressure. Am J Physiol Heart Circ Physiol. 2011; 301(3):H964–H974. [PubMed: 21724863]
25. Girouard SD, Rosenbaum DS. Role of wavelength adaptation in the initiation, maintenance, and pharmacologic suppression of reentry. J Cardiovasc Electrophysiol. 2001; 12(6):697–707. [PubMed: 11405405]
26. Flagg TP, Patton B, Masia R, Mansfield C, Lopatin AN, Yamada KA, et al. Arrhythmia susceptibility and premature death in transgenic mice overexpressing both SUR1 and Kir6.2[DeltaN30, K185Q] in the heart. Am J Physiol Heart Circ Physiol. 2007; 293(1):H836–H845. [PubMed: 17449558]
27. Lammers WJ, Kirchhof C, Bonke FI, Allessie MA. Vulnerability of rabbit atrium to reentry by hypoxia. Role of inhomogeneity in conduction and wavelength. Am J Physiol. 1992; 262(1 Pt 2):H47–H55. [PubMed: 1733321]
28. Coronel R, Janse MJ, Opthof T, Wilde AA, Taggart P. Postrepolarization refractoriness in acute ischemia and after antiarrhythmic drug administration: action potential duration is not always an index of the refractory period. Heart Rhythm. 2012; 9(6):977–982. [PubMed: 22293142]
29. Saito T, Sato T, Miki T, Seino S, Nakaya H. Role of ATP-sensitive K + channels in electrophysiological alterations during myocardial ischemia: a study using Kir6.2-null mice. Am J Physiol Heart Circ Physiol. 2005; 288(1):H352–H357. [PubMed: 15598870]
30. Fukuzaki K, Sato T, Miki T, Seino S, Nakaya H. Role of sarcolemmal ATP-sensitive K + channels in the regulation of sinoatrial node automaticity: an evaluation using Kir6.2-deficient mice. J Physiol. 2008; 586(Pt 11):2767–2778. [PubMed: 18420708]
31. Maruyama M, Joung B, Tang L, Shinohara T, On YK, Han S, et al. Diastolic intracellular calcium-membrane voltage coupling gain and postshock arrhythmias: role of purkinje fibers and triggered activity. Circ Res. 2010; 106(2):399–408. [PubMed: 19926871]
32. Gumina RJ, O'Cochlain DF, Kurtz CE, Bast P, Pucar D, Mishra P, et al. KATP channel knockout worsens myocardial calcium stress load in vivo and impairs recovery in stunned heart. Am J Physiol Heart Circ Physiol. 2007; 292(4):H1706–H1713. [PubMed: 17189350]
33. Baczko I, Jones L, McGuigan CF, Manning Fox JE, Gandhi M, Giles WR, et al. Plasma membrane KATP channel-mediated cardioprotection involves posthypoxic reductions in calcium overload and contractile dysfunction: mechanistic insights into cardioplegia. FASEB J. 2005; 19(8):980–982. [PubMed: 15774423]
34. Nichols CG, Ripoll C, Lederer WJ. ATP-sensitive potassium channel modulation of the guinea pig ventricular action potential and contraction. Circ Res. 1991; 68(1):280–287. [PubMed: 1984868]
35. Baczko I, Husti Z, Lang V, Lepran I, Light PE. Sarcolemmal KATP channel modulators and cardiac arrhythmias. Curr Med Chem. 2011; 18(24):3640–3661. [PubMed: 21774762]
36. Fedorov VV, Glukhov AV, Ambrosi CM, Kostecki G, Chang R, Janks D, et al. Effects of KATP channel openers diazoxide and pinacidil in coronary-perfused atria and ventricles from failing and non-failing human hearts. J Mol Cell Cardiol. 2011; 51(2):215–225. [PubMed: 21586291]
37. D'Hahan N, Moreau C, Prost AL, Jacquet H, Alekseev AE, Terzic A, et al. Pharmacological plasticity of cardiac ATP-sensitive potassium channels toward diazoxide revealed by ADP. Proc Natl Acad Sci U S A. 1999; 96(21):12162–12167. [PubMed: 10518593]
38. Isidoro Tavares N, Philip-Couderc P, Papageorgiou I, Baertschi AJ, Lerch R, Montessuit C. Expression and function of ATP-dependent potassium channels in late post-infarction remodeling. J Mol Cell Cardiol. 2007; 42(6):1016–1025. [PubMed: 17512536]

39. Koumi SI, Martin RL, Sato R. Alterations in ATP-sensitive potassium channel sensitivity to ATP in failing human hearts. Am J Physiol. 1997; 272(4 Pt 2):H1656–H1665. [PubMed: 9139948]

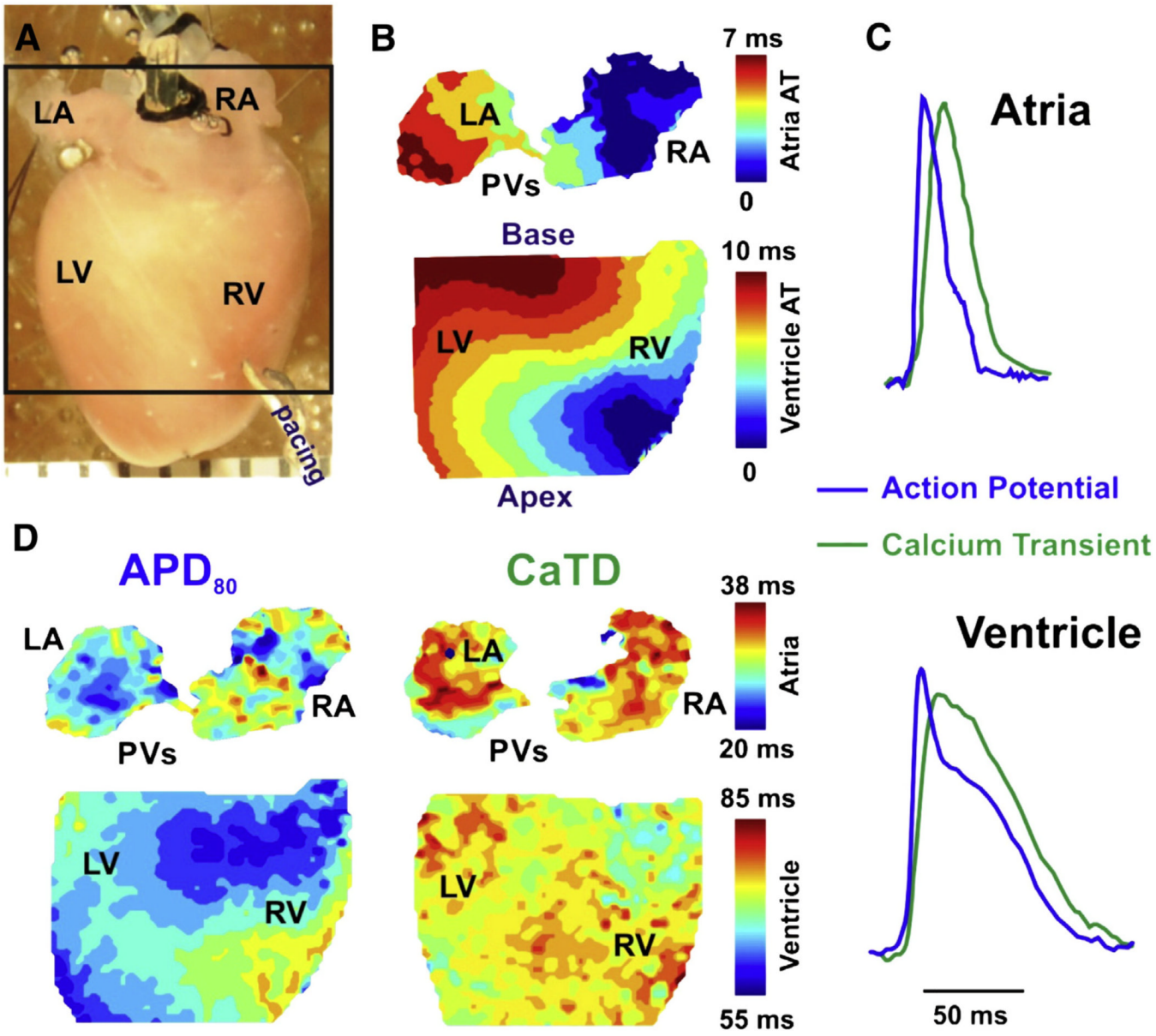

Fig. 1.

Experimental set up. A: The posterior surface of Langendorff-perfused mouse hearts was optically mapped during MI using voltage (RH237) and calcium (Rhod-2) sensitive fluorescent dyes with a CMOS Ultima-L camera. B: Activation maps were constructed from activation times (AT) determined from the dV/dt_{max}. C: Representative examples of superimposed optical recordings of AP (blue) and calcium transient (green) signals measured in mouse atria (top) and ventricle (bottom). D: Contour maps for the distribution of action potential duration (APD) and calcium transient duration (CaTD) at 80% return to baseline fluorescence are shown. (RA and LA – right and left atria; RV and LV – right and left ventricles; PVs – pulmonary veins). (For interpretation of the references to color in this figure legend, the reader is referred to the web version of this article.)

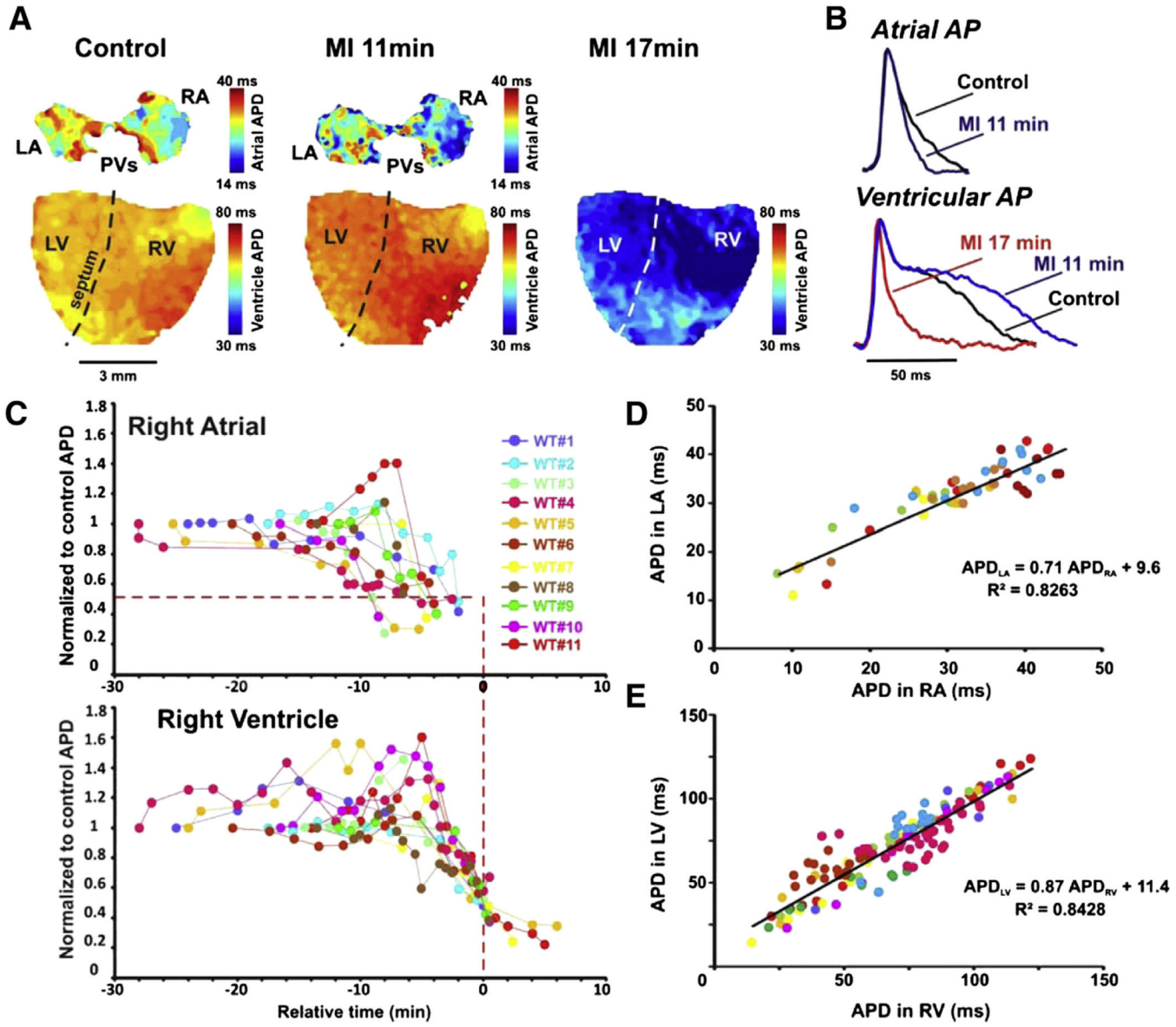

Fig. 2.

APD changes in WT mice during MI. A: Representative APD maps for a WT heart in control, 11 min into MI, and 17 min into MI. The color bar to the right of the images represents the APD in individual pixels from short (blue) to long (red). B: Representative AP traces from the atria (top) and ventricle (bottom) in control (black), 11 min MI (blue) and 17 min MI (red). C: RA and RV APD during MI from WT hearts (n = 11, each color represents a specific heart). Relative time (T_{rel}) of 0 is defined as the time at which ventricular APD reaches 50% shortening (represented by red vertical dashed line). This relative time shift has been applied for all paired ventricular and atrial APD traces. Note that in all paired APD traces, the atrial APD shortens to 50% of control values (horizontal red dotted line) before T_{rel} = 0. D and E: Correlation between APDs measured in LA and RA (D) and between LV and RV (E), throughout MI. Individual colors as in (C).

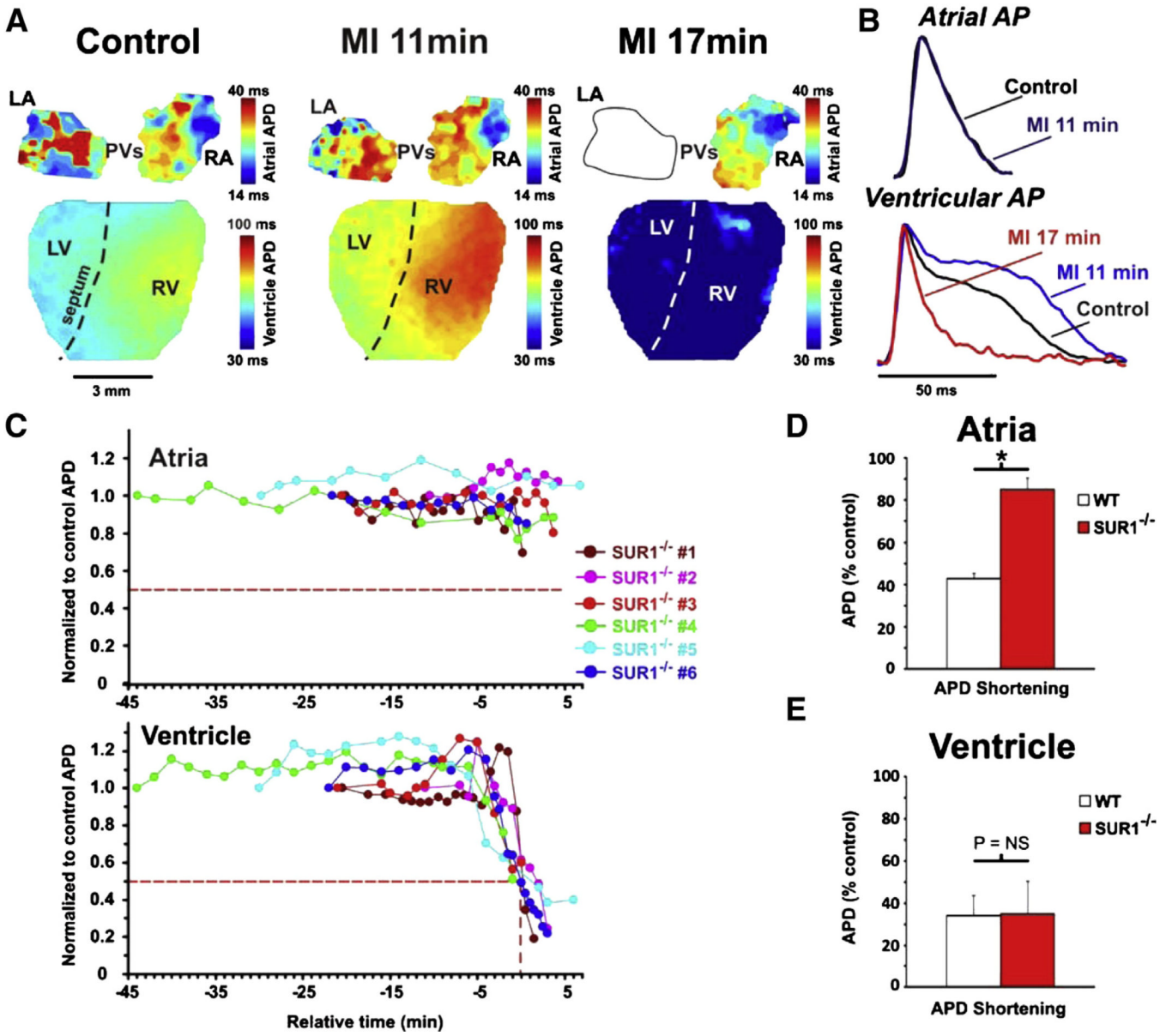

Fig. 3.

APD changes in SUR1$^{-/-}$ mice during MI. A: Representative APD maps for a SUR1$^{-/-}$ heart in control, 11 min MI, and 17 min MI. The ventricle responds in a similar manner to WT ventricles. The atria do not show shortening at 11 min MI. By 19 min, conduction to the LA was blocked but the RA still does not show APD shortening. B: Representative AP traces from atria (top) and ventricle (bottom) from control (black), 11 min MI (blue), and 17 min MI (red). Ventricles show a longer APD plateau at 11 min and a drastic shortening by 17 min. C: Representation of the atrial (top) and ventricular (bottom) APDs during MI from SUR1$^{-/-}$ hearts (n = 6) with relative time as in Fig. 2. The atria show no significant shortening relative to the control APD throughout MI but the ventricles display a similar biphasic effect as that seen in WT mice. D: Quantification of the relative APD shortening in WT and SUR1$^{-/-}$ atria during MI shows a clear shortening in WT but not SUR1$^{-/-}$ atria. E: Quantification of the relative APD shortening in WT and SUR1$^{-/-}$ ventricle during MI reveals no differences in the ventricles.

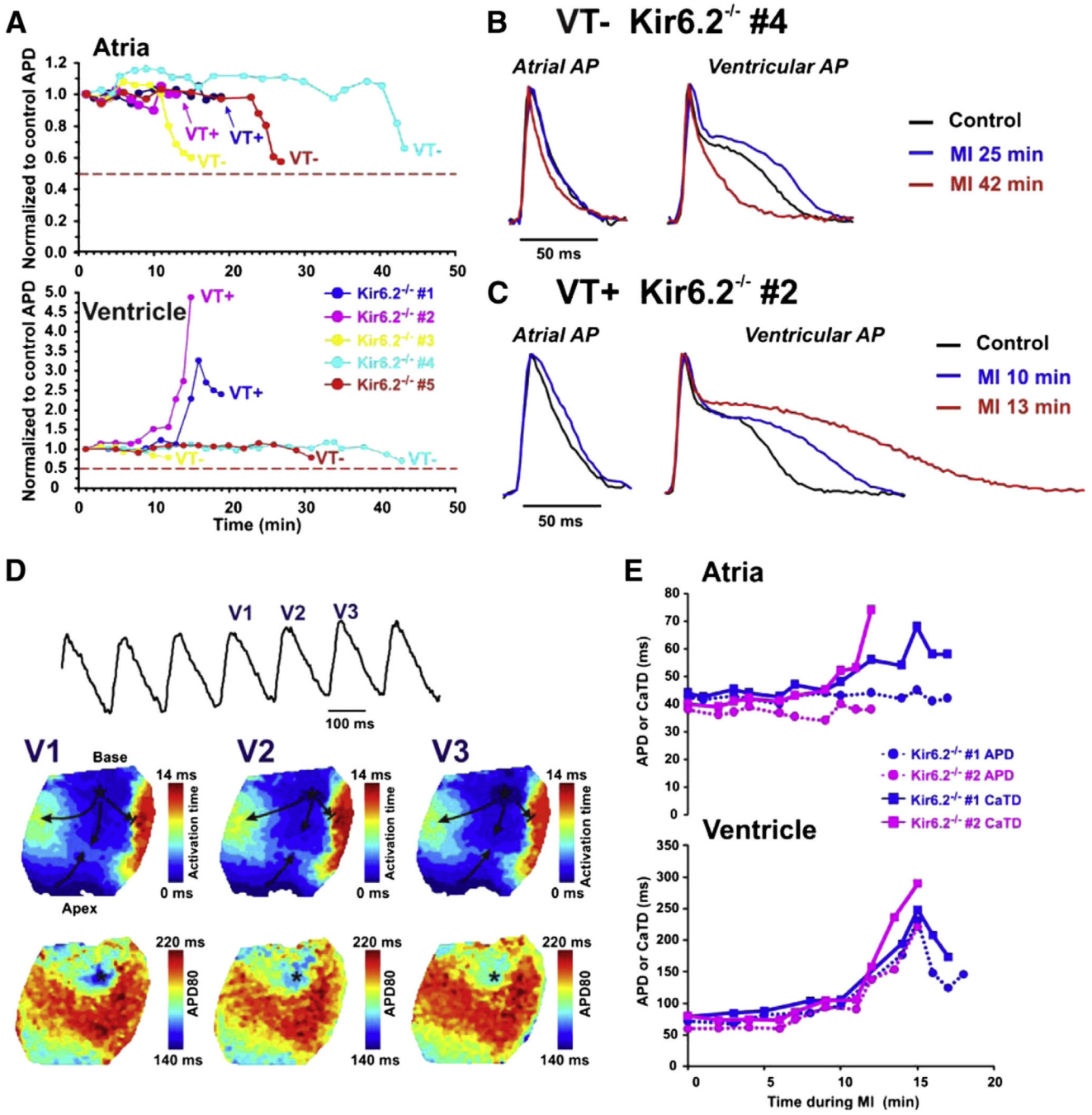

Fig. 4.

APD changes in Kir6.2$^{-/-}$ mice during MI. A: Relative changes in APD during MI in atria (top) and ventricle (bottom). Two of five Kir6.2$^{-/-}$ hearts displayed severe APD prolongation in ventricles and developed both ventricular and atrial tachycardia (labeled VT +) during MI. The other three Kir6.2$^{-/-}$ hearts (labeled as VT− group) displayed a relatively stable ventricular APD but some shortening of the APD in very late MI. Notably, none of the Kir6.2$^{-/-}$ atria or ventricle displayed APD shortening of more than 50% of their control values. B and C: Representative APs recorded in atria and ventricle of VT− (B) and VT+ (C) Kir6.2$^{-/-}$ hearts in control and during MI. D: Representative example of ventricular tachycardia recorded in VT+ Kir6.2$^{-/-}$ heart during late MI. Representative trace of

ventricular AP recorded during VT is shown. V1, V2 and V3 are mapped VT waves. Below are the activation (top) and APD distribution (bottom) contour maps reconstructed for the mapped VT waves (V1–V3). Stable location of the earliest activation area is marked by an asterisk which corresponds to the region with the shortest APD. Arrows demonstrate the direction of propagation. E: APD (circle, dotted trace) and CaTD (square, solid trace) measurements during MI for the 2 VT+ Kir6.2$^{-/-}$ hearts are presented for atria and ventricle.

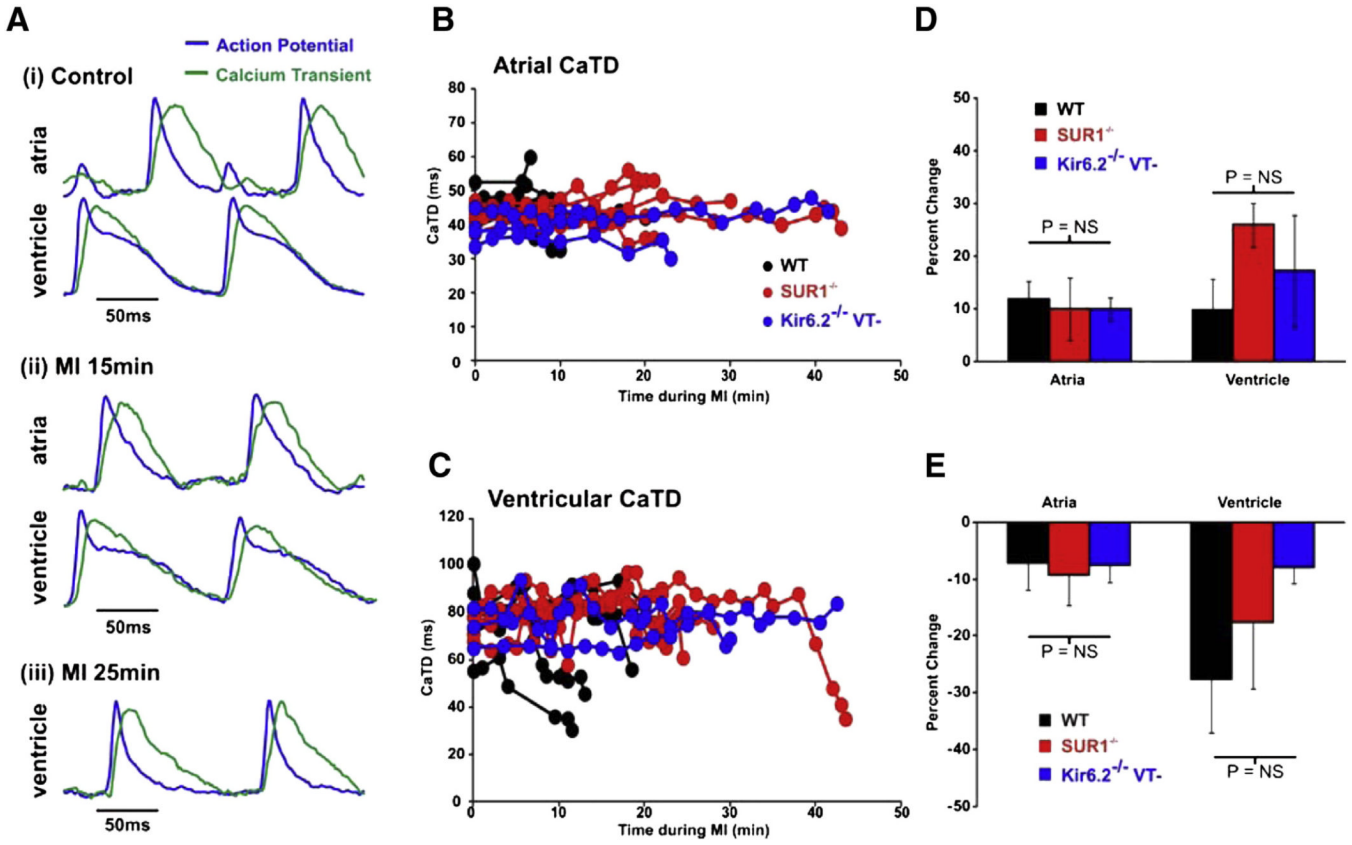

Fig. 5.

Calcium transient changes in WT and SUR1$^{-/-}$ mice during MI. A: Representative optical recordings of AP (blue) and CaT (green) signals obtained from the LA and LV of a SUR1$^{-/-}$ heart (i) in control, (ii) during 15 min and (iii) 25 min of MI. B and C: CaTD in atria (B) and ventricles (C) of WT, SUR1$^{-/-}$, and VT− Kir6.2$^{-/-}$ hearts during MI. D and E: Maximal CaTD prolongation during MI (D) and CaTD shortening (E) in each group.

Table 1

Control APD values (average APD ± STDEV).

	Left atria	Right atria	Left ventricle	Right ventricle
WT	34.4 ± 5.4 ms	33.6 ± 2.7 ms	74.4 ± 13.0 ms	69.2 ± 13.9 ms
$SUR1^{-/-}$	35.7 ± 3.8 ms	34.4 ± 4.3 ms	82.6 ± 7.0 ms	80.6 ± 5.8 ms
$Kir6.2^{-/-}$	32.6 ± 2.2 ms	36.8 ± 4.2 ms	74.3 ± 12.0 ms	76.4 ± 14.7 ms

Table 2

Control CaTD values (average CaTD ± STDEV).

	Left atria	Right atria	Ventricle
WT	42.0 ± 2.7 ms	44.5 ± 5.3 ms	79.5 ± 17.3 ms
$SUR1^{-/-}$	43.3 ± 3.0 ms	43.3 ± 2.7 ms	74.9 ± 5.0 ms
$Kir6.2^{-/-}$	39.7 ± 4.7 ms	40.1 ± 3.6 ms	76.1 ± 6.9 ms